The Japan Society
of Applied Physics

PROGRESS REVIEW • OPEN ACCESS

Toward 2D grating coupler enabled O-band coherent links based on SiGe photonic electronic technology

To cite this article: Lars Zimmermann *et al* 2023 *Jpn. J. Appl. Phys.* **62** SC0807

View the article online for updates and enhancements.

PROGRESS REVIEW

Toward 2D grating coupler enabled O-band coherent links based on SiGe photonic electronic technology

Lars Zimmermann[1,2]* , Pascal M. Seiler[1,2] , Christian Mai[2], and Galina Georgieva[3]

[1]Technische Universitaet Berlin, FG Siliziumphotonik, HFT4, Einsteinufer 25, D-10587 Berlin, Germany
[2]IHP–Leibniz-Institut f. innovative Mikroelektronik, Im Technologiepark 25, D-15236 Frankfurt (Oder), Germany
[3]Technische Universitaet Berlin, Hochfrequenztechnik-Photonik, HFT4, Einsteinufer 25, D-10587 Berlin, Germany

*E-mail: l.zimmermann@tu-berlin.de

Coherent techniques for short reach intra-datacenter optical interconnects are currently intensely discussed. This article reports progress on previous work that analyzed the benefits of switching from C- to O-band optics with regard to digital signal processing. Here we study the feasibility of adapting a coherent approach to an established datacenter interconnect technology (PSM4). This PSM4-like implementation brings about the benefit of much improved resilience to laser drift, thus reducing or eliminating the need for a temperature stabilized laser, which is typically assumed a requirement for coherent transceivers. The analysis rests on simulation parameters derived in part from previous experimental realizations of coherent receivers in SiGe photonic BiCMOS technology. In addition, we make use of recent results regarding the optimization of O-band 2D grating couplers with respect to efficiency and low polarization dependence over a 20 nm wavelength window. We identify such couplers as enabling building blocks for coherent PSM4-like implementations. © 2023 The Author(s). Published on behalf of The Japan Society of Applied Physics by IOP Publishing Ltd

1. Introduction

Silicon photonics is a prominent contender among the technological approaches employed for photonic integrated circuits for data center interconnects. Major advantages of this technology are related to meeting the increased cost pressure, the need for scalable solutions (i.e. large substrates), and a technology base for rapid development cycles matching industry requirements. With increasing line-rates an additional advantage receives renewed attention, the possibility of close proximity co-integration of RF transistors and silicon photonic phase-shifters and photodiodes to realize high-speed electronic amplification and driving with minimum parasitics. This had been the initial driver of photonic BiCMOS development.[1,2] SiGe:C-based hetero-junction bipolar transistors (HBT) have a track record in RF frontends for optical communications. Particularly advantageous are f_T/f_{max} values reaching 500 GHz and beyond, while breakdown voltages stay ahead of conventional CMOS. Photonic BiCMOS monolithically integrates RF SiGe:C BiCMOS electronics (npn HBT + CMOS) with 220 nm SOI silicon photonics, including high-speed waveguide integrated germanium photodiodes,[3] enabling single-chip C- and O-band Tx and Rx sub-systems. Recently, there is increasing interest in O-band coherent interconnects inside the data center targeting shorter links with capacity of 1.6 Tbit s^{-1} or beyond. While the general pros and cons of digital coherent technology on short reach links are being debated, it is clear that coherent O-band links require a novel class of coherent transceivers based on high-performance integrated optics and opto-electronics. To better understand the transceiver requirements, it is useful to start from an existing data center short reach link implementation (e.g. PSM4, DR4 or FR4) and adapt it to coherent technology building blocks. In this article, we shall present a numerical analysis of a PSM4-like coherent link, setting the requirement margins for the optical fiber interface in terms of efficiency, but especially polarization handling capability. Following, we shall present our recent progress regarding design and fabrication of such 2D grating couplers (2D-GRC).

2. Numerical analysis of PSM4-like coherent link

Critical for a successful mass market entry of coherent technology in the intra data center domain is a significant reduction in power consumption. This is required in order to be competitive with present direct-detect solutions. Here, significant power savings are achieved through three key enablers: (1) by implementing O-band coherent links, rather than conventional C-band solutions, digital signal processing (DSP) dedicated to the compensation of chromatic dispersion (CD) can be completely removed.[4] (2) Typically, temperature control is required for coherent transceivers to stabilize the lasers' emission wavelength, limiting the beating between modulated signal and local oscillator (LO). This is crucial not only to avoid inter channel crosstalk between multiple wavelength division multiplexing channels, but also to efficiently utilize the limited optical-electrical receiver bandwidth. This is tremendously relaxed in a self-homodyne parallel single-mode fiber (PSM) scheme, since signal and LO originate from the same source, thus exhibiting the same long term wavelength drift and short term phase noise. Drawback is the necessity to transmit the LO in parallel to the PSM signals in a dedicated single-mode fiber, as well as additional splitting of signal/LO on transmit/receive side. (3) Dedicated device optimization to improve the overall power budget. Here we investigate the benefits resulting from the utilization of high-performance 2D-GRCs, featuring back-side reflectors for improved coupling efficiencies. Such devices are presently being developed and will be discussed in greater detail in the following section. Grating coupler design targets are minimum −4 dB coupling efficiency and maximum 0.5 dB polarization dependence.

Another critical device for the optical link is the modulator. All-silicon Mach–Zehnder modulators frequently show opto-electrical bandwidth <50 GHz, large modulation loss and half-wave voltage V_π and considerable power consumption.[5] For these reasons, we consider the realization of Pockels modulator based on hybrid integration approach mandatory. A successful integration of a BaTiO3-based modulator on our platform took already place in the past.[6] However, further design and technological developments are necessary. For the following simulations, a Pockels modulator with state-of-the-art characteristics is presumed.

2.1. Simulation setup

An outline of the PSM concept is given in Fig. 1. The feasibility of this approach is evaluated with the aid of Monte-Carlo simulations[7] implemented in MATLAB using the parameters given in Table I. Alternative means regarding the simulation-aided performance evaluation of coherent links include the analytical evaluation of a theoretical SNR.[8,9] In order to support 1.6 Tbit s^{-1} aggregate data rate, four parallel transmit channels, each operating at 400 Gbit s^{-1}, are required. Therefore, 60 GBaud DP-QAM16 is chosen as symbol rate and modulation format, enabling 480 Gbit s^{-1} per channel. The overhead in excess of 400 Gbit s^{-1} accounts for potential implementations of forward error correction. Hereinafter, we only consider one of the four PSM channels for the simulation.

Unless stated otherwise, an optical output power of +20 dBm and a relative intensity noise (RIN) of −140 dB Hz^{-1} is assumed for the simulation. As optical interfaces we use simulated 2D-GRC characteristics optimized for our photonic BiCMOS technology, similarly obtained recently.[10] The fabrication process for O-band 2D-GRCs is presently still under development. Since the process optimization for realizing the perturbing elements' geometry is still ongoing, we rely on simulated results (2D-GRCs with back-reflector, see Sect. 3). To account for the 2D-GRC's polarization-dependent loss (PDL), we use the worst-case coupling efficiency for all simulations. Subsequently to chip-coupling, the light is split into signal and LO at a varied split ratio. On the transmit side, the signal is furthermore split by 6 dB, thus separating the signal into four independent PSM channels. The IQ modulator is modeled as a nested IQ Mach–Zehnder-modulator, featuring an individual 3 dB bandwidth of 50 GHz and 2.5 dB optical propagation loss. Following out-coupling of the five signals (four modulated PSM channels, one LO), a variable attenuator is added in the simulation. By varying the attenuation, the total link loss budget, supporting fiber optical propagation loss and optical circuit switching,[11] may be determined. On the receive side, the LO is split by 6 dB, accommodating the four PSM channels. The O-band coherent receiver is modeled after reported devices, fabricated in our photonic BiCMOS technology.[12,13] Unknown parameters, e.g. photodiode (PD) and transimpedance amplifier (TIA) characteristics, are based on typical technology parameters and electrical performances. For the 90° hybrid, simulated characteristics obtained for the hybrid used within the fabricated receiver are implemented.[13] Lastly, the TIA outputs are quantized by 4 bit analog-to-digital converters (ADCs) and DSP is applied for bit-error-rate calculation. The DSP includes matched filtering, normalization, and adaptive equalization based on a least-mean-squares algorithm.

2.2. Numerical results

The end-to-end link modeling focuses chiefly on three system-related parameters, namely wavelength dependencies, laser launch power, and LO/signal split ratio. Firstly, the link loss budget in a 20 nm window, i.e. from 1310 to 1330 nm, has been investigated for varied LO/signal split ratios. The beating between modulated PSM signal and LO is minimized due both originating from the same source in a self-homo-dyne PSM scheme. However, uncooled lasers will exhibit a long term emission wavelength drift due to temperature-dependent refractive index changes, which causes variations in the coupling efficiency and thus overall link performance. Note that variations in fiber's optical propagation loss can be reasonably neglected at link distances of just a few kilo-meters, and the 1 dB loss bandwidth of the 90° hybrid is approximately[13] 50 nm, and thus significantly larger than the 2D GRC's 1 dB bandwidth (comp. Sect. 3). Results for the end-to-end link modeling at varied emission wavelengths are given in Fig. 2(a), whereat different wavelengths account for the coupling efficiency variation of the 2D-GRC. In terms of maximizing the link loss budget, an ideal LO-to-signal split ratio of 50% can be identified. This is independent of the modulator's insertion loss, as it is the result of maximizing the signal-to-noise ratio at the coherent receiver.[14] Assuming an ideal 3 dB LO/signal splitting, a link loss budget of 3–6 dB in a 20 nm window can be expected based on Fig. 2(a). This is sufficient to support the fiber propagation loss of a few kilometers, while the excess budget may be used for optical circuit switching,[11] or integrated polarization controlling.[14] It should be noted that the loss budget is guaranteed only with the required modulator characteristics.

Naturally, the link loss budget is largely depending on the laser optical output power as well. An analysis of the impact of laser launch powers between +18 dBm and +20 dBm is given in Fig. 2(b). While a higher laser output power naturally leads to a higher link loss budget, it needs to be noted that other effects presently not covered by the simula-tion, e.g. stimulated Brillouin scattering (SBS), may
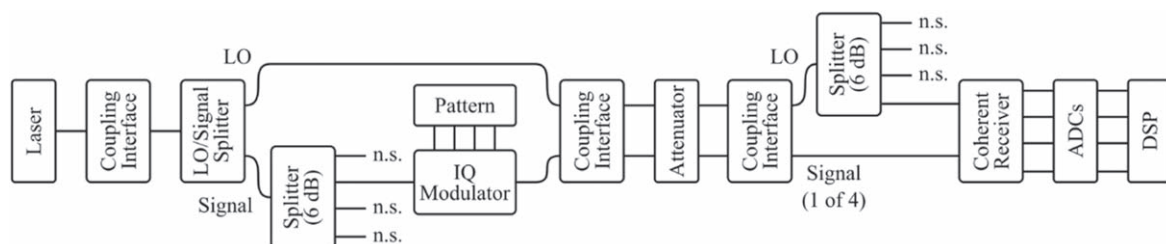
Fig. 1. O-band coherent intra datacenter interconnect based on a PSM approach (one direction). Only one of four transceiver links is shown in detail. n.s.: not shown, ADC: analog-to-digital converter, DSP: digital signal processing, LO: local oscillator.

Table I. List of simulation parameters.

Parameter	Value	Parameter	Value
Laser power (before chip coupling and splitting)	+20 dBm	Laser RIN	−140 dB Hz^{-1}
MZM bandwidth (−3 dB)	50 GHz	MZM optical prop. loss	2.5 dB
Modulation depth Vpp/Vpi	1.0	Internal PD responsivity	0.7 A W^{-1}
PD bandwidth (−3 dB)	53 GHz	PD dark current	100 nA
TIA input-referred noise current density	24 pA/√Hz	TIA bandwidth (−3 dB)	30 GHz
Symbol rate	60 GBaud	Modulation format	DP-QAM16
ADC resolution	4 bit		
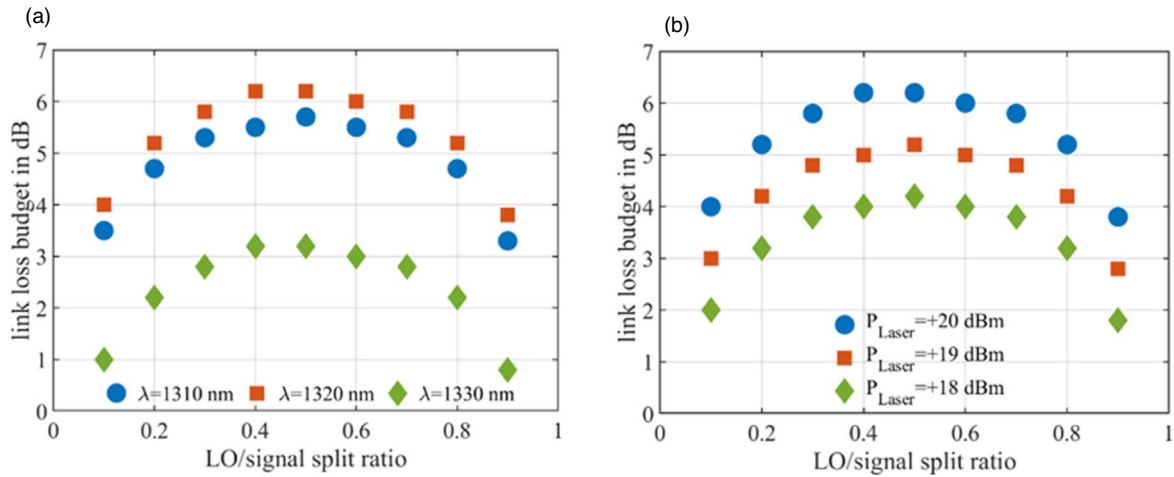
Fig. 2. (Color online) Simulated end-to-end link performance. (a) Link loss budget at a laser output power of +20 dBm at varied LO/signal split ratios and a target BER of 4.5E-3. (b) Link loss budget at 1320 nm and varied laser optical output powers for varied LO/signal split ratios and a target BER of 4.5E-3.

negatively affect the system performance.[14] Potential solutions for self-homodyne systems to overcome that limitation include larger linewidth laser sources and a reduction of optical power coupled to the LO path, whereby the latter approach operates the system in a sub-optimal mode.[14] An increase in linewidth is difficult to realize, as laser linewidth and length mismatch between signal and LO display a critical system parameter in self-coherent schemes.[9] A reduction of LO power launched into the fiber link may be achieved by shifting the LO PSM splitting from the receive to the transmit side. However, this also increases the number of transmitted signals per direction from five to eight, thus requiring a total of 16 fibers for up- and downstream. A bi-directional PSM approach could be implemented[14] to limit the amount of fibers required for up- and downstream. The self-coherent PSM scheme analyzed in this section may be further extended towards potential dual-band coherent applications,[15] but further investigations regarding that application are required.

3. Optimization of two-dimensional grating couplers in 0.25 μm photonic BiCMOS technology

Component optimization for coherent receivers lead to adequate performance already several years ago.[16,17] However, as already indicated in the previous section, there are still stringent requirements for the development of coupling interfaces, which will be used in a low-cost optical link. Independent of the modulation scheme (intensity or quadrature amplitude modulation), the optical coupler should be able to fulfill several criteria. On the one hand, general

aspects relevant to the accomplishment of the complete assembly have to be considered,[18] i.e.:

- Automated wafer-level testing capability, during different manufacturing steps.
- Reasonable demands on the packaging precision.

Presently, 2D-GRCs are the more advanced interface in silicon photonic sub-systems, compared to horizontal coupling solutions. For this reason, substantial efforts have been made to optimize such structures, considering the boundary conditions of a 0.25 μm photonic BiCMOS technology (248 nm DUV lithography). Particularly, the design development targets at the performance specifications outlined in the previous section, namely:

- Low insertion loss: at least 4 dB per polarization is desirable, potential laser emission drift has to be considered.
- Low PDL: the difference between the maximal and minimal coupling efficiency for different received polarizations should be < 0.5 dB.

Especially the latter aspect is a substantial challenge for 2D-GRCs. It is well known that 2D-GRCs with circular perturbing elements exhibit a strong polarization dependence.[19,20] The effect is mostly caused by a spectral shift between two orthogonal polarization states. In simulations, we consider as extreme cases the polarization states, which are decomposed by the grating into components with an even or odd symmetry. Accordingly, the polarization states are assigned as an even- and odd-polarization [see Fig. 3(a)]. To illustrate this issue, we simulated a 2D-GRC designed for our technology with the following parameters:
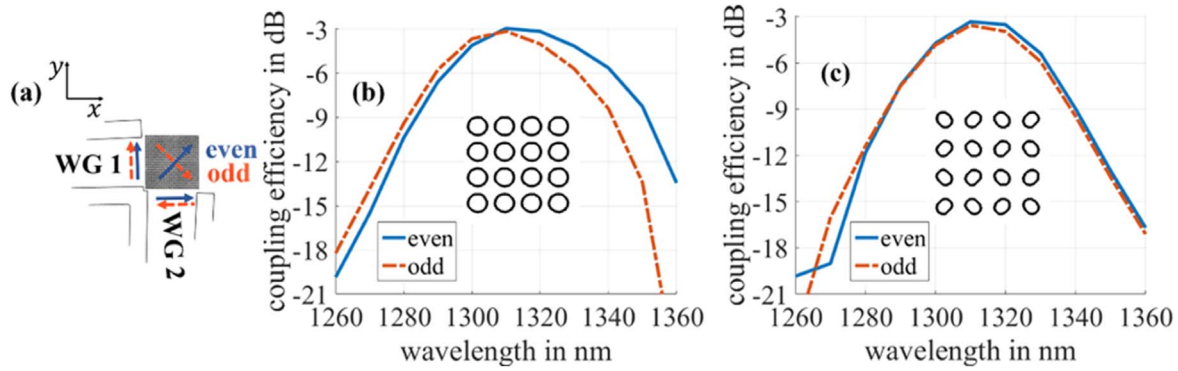
Fig. 3. (Color online) (a) Definition of an even- and odd-polarization. Simulated coupling spectra of the even- and odd-polarization for (b) a 2D-GRC with circular perturbing elements (c) a 2D-GRC with zig-zag tilted oval perturbing elements.

- Rib waveguides: 220 nm Si on 2 μm SiO$_2$ with a slab width of 2 μm and slab etch depth equal to the grating etch depth. The waveguides are tilted with respect to the grating plane by a waveguide-to-grating shear angle[21–23] of 2°.
- Grating: etch depth of 120 nm, grating period of 480 nm, circular perturbing elements with a diameter of 280 nm. The coupling angle at the symmetry plane is 8°.

Figure 3(b) shows the coupling efficiency in the even and odd case. The PDL exceeds 0.5 dB for wavelengths others than 1310 nm. Although the component has a reasonable coupling efficiency of −3 dB at 1310 nm with a 1 dB-bandwidth of about 20 nm, the wavelength-dependent PDL makes it highly sensitive against drifts of the emission wavelength of uncooled lasers.

The PDL optimization of 2D-GRCs requires a deep understanding of the physics behind the polarization interactions within the grating. During the recent years, we were concerned with the investigation of phenomena related to polarization crosstalk. At first, we analyzed the orthogonal polarization conversion, i.e. the cross-polarization in 2D-GRCs.[24] For instance, if we have a y-polarized input field (target-polarization), the 2D-GRC converts it partially to an x-polarized field, assigned as a cross-polarization. While we found[24] that the cross-polarization scales with the grating's perturbation strength (thus, limiting the coupling efficiency), we indicated in-plane scattering as its physical origin.[25] The latter is caused by the finite size of the grating perturbing elements with respect to the incident optical field. The presence of in-plane scattering and thus of cross-polarization is the main reason for PDL in 2D-GRCs. This can be explained by the fact that for different incident fields, a given target-polarization is superposed with the cross-polarized signal originating from the other channel with a different phase relation. If we consider again the even- and odd-polarizations in Fig. 3(a), in the even case the target-polarization is superposed with the cross-polarization in-phase. By contrast, the target- and cross-polarization are combined in anti-phase in the odd case. This is the reason for the different spectra of the even- and odd-polarization in Fig. 3(b).

The elimination of in-plane scattering and cross-polarization is not a trivial task, especially with the constraints given by our 0.25 μm photonic BiCMOS. The realization of customized perturbing elements[19,26–29] is not easily implementable in this technology. This made the development of

alternative solutions necessary. We demonstrated[10] for the first time a novel optimization technique to realize 2D-GRC with a low cross-polarization and low PDL—the zig-zag tilted ovals grating. The application of this method in O-band can be done in analogous way, resulting in an exemplary geometry with the parameters:

- Rib waveguides: 220 nm Si on 2 μm SiO$_2$ with a slab width of 2 μm and slab etch depth equal to the grating etch depth. The waveguides are tilted with respect to the grating plane by a waveguide-to-grating shear angle of 2°.
- Grating: etch depth of 140 nm, grating period of 480 nm, oval perturbing elements with a short diameter of 180 nm and a long diameter of 260 nm. The coupling angle at the symmetry plane is 8°.

The coupling spectra of the even- and odd-polarization for the optimized design are given in Fig. 3(c), showing a substantial improvement of the PDL, while keeping the coupling efficiency and the 1 dB-bandwidth almost unaffected (−3.3 dB at 1310 nm and 20 nm resp.). The PDL is below 0.5 dB within the complete 1 dB-bandwidth, which guarantees good device robustness against laser spectral drifts. In addition, the optimized design eliminates issues related to polarization crosstalk in polarization-multiplexed systems.[30] Further improvement of the 2D-GRC coupling efficiency can be considered by using a metal mirror below the grating, acting as a back-reflector.[26,29,31] Figure 4 shows the coupling spectra of the even- and odd- polarization for the same optimized design, simulated with a metal back-reflector. Due to changes in the out-coupled power, the spectra appear
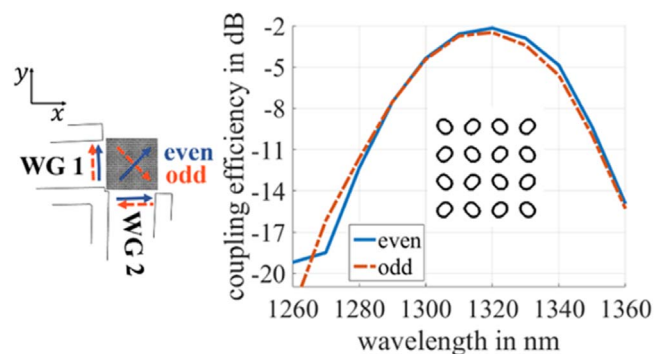
Fig. 4. (Color online) Simulated coupling spectra of the even- and odd-polarization for a 2D-GRC with zig-zag tilted oval perturbing elements and a back-side reflector.
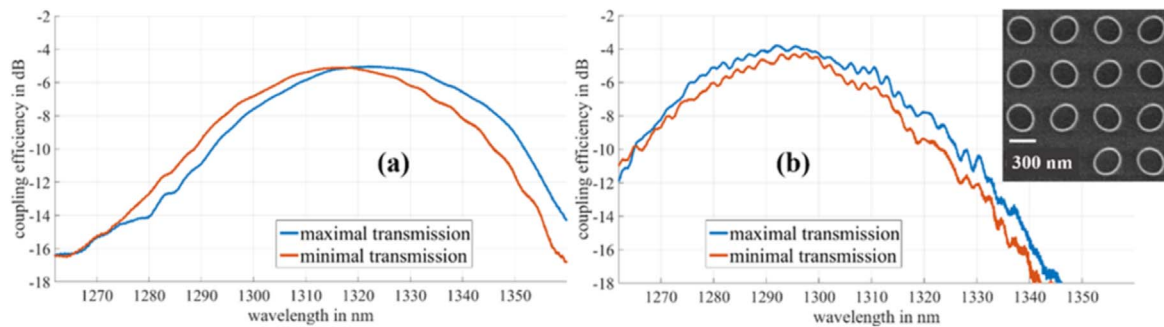
Fig. 5. (Color online) Measured coupling spectra of polarizations, resulting in a minimal or maximal transmission. (a) 2D-GRC with circular perturbing elements. (c) 2D-GRC with zig-zag tilted oval perturbing elements.

slightly shifted. We observe no deterioration in terms of PDL and 1 dB-bandwidth, while in the same time the coupling efficiency improves by about 1 dB (maximum -2.2 dB at 1320 nm). The simulation results confirm the feasibility of the optimization technique for 2D-GRCs in low-cost optical links.

Our current work is focused on the fabrication improvement of zig-zag tilted ovals 2D-GRCs for O-band. The first-generation 2D-GRCs already shows a PDL improvement, compared to the gratings with circular perturbing elements [see Figs. 5(a) and 5(b)]. However, the desired perturbing elements dimensions are still not realized with the required accuracy and robustness, making the investigation of more appropriate shape biases still necessary.

4. Conclusions

In this article we studied the feasibility of adapting existing short reach datacenter interconnect technology (PSM4, presently using O-band direct detect technology) to coherent O-band technology. The major aspects of this work concern a numerical analysis of the respective link loss budget and an investigation of 2D-GRC based efficient fiber chip coupling with very low polarization dependence. Our analysis indicates that the previously introduced zig-zag 2D -GRC design is needed to achieve positive link loss budget. However, the reached power budgets require the deployment of a modulator with sufficiently good characteristics in terms of propagation loss, bandwidth and half-wave voltage V_{π}. Our analysis points toward the need of an efficient phase shifter implementation such as the mentioned Pockels phase shifters that would allow for lower optical propagation losses while also enabling low half-wave voltages, which further reduces the optical insertion loss.

ORCID iDs

Lars Zimmermann https://orcid.org/0000-0002-0927-4986
Pascal M. Seiler https://orcid.org/0000-0001-8553-3137
Galina Georgieva https://orcid.org/0000-0003-2693-8147

1) L. Zimmermann et al., "Silicon photonics front-end integration in high-speed 0.25 μm SiGe BiCMOS," 5th IEEE Int. Conf. on Group IV Photonics, p. 374, 2008, 10.1109/GROUP4.2008.4638204.
2) L. Zimmermann et al., "Monolithically integrated 10 Gbit s^{-1} silicon modulator with driver in 0.25 μm SiGe: C BiCMOS," 39th European Conf.
3) S. Lischke, D. Knoll, C. Mai, and L. Zimmermann, "Advanced photonic BiCMOS technology with high-performance Ge photo detectors," Proc. SPIE **11088**, 110880M (2019).
4) P. M. Seiler and L. Zimmermann, "Power efficiency improvements in coherent O-band data center interconnects," Photonics in Switching and Computing 2021, paper Tu4C.3, 2021, 10.1364/PSC.2021.Tu4C.3.
5) D. Petousi et al., "Performance limits of depletion-type silicon Mach–Zehnder modulators for telecom applications," J. Lightwave Technol. **31**, 3556 (2013).
6) F. Eltes et al., "A BaTiO$_3$-based electro-optic pockets modulator monolithically integrated on an advanced silicon photonics platform," J. Lightwave Technol. **37**, 1456 (2019).
7) W. H. Tranter, K. Sam Shanmugan, T. S. Rappaport, and K. L. Kosbar, *Principles of Communication Systems Simulation with Wireless Applications* (Prentice Hall, Upper Saddle River, NJ, 2004).
8) B. Zhang, C. Malouin, and T. J. Schmidt, "Design of coherent receiver optical front end for unamplified applications," Optics Express **20**, 3225 (2012).
9) G. Rizzelli, A. Nespola, S. Straullu, F. Forghieri, and R. Gaudino, "Phase noise impact and scalability of self-homodyne short-reach coherent transmission using DFB lasers," J. Lightwave Technol. **40**, 37 (2022).
10) G. Georgieva, P. M. Seiler, C. Mai, A. Peczek, K. Petermann, and L. Zimmermann, "A polarization-independent zig-zag-tilted ovals grating coupler in a 0.25 μm photonic BiCMOS technology," 2022 European Conf. on Optical Communications (ECOC), paper Mo3F.5, 2022.
11) L. Poutievski et al., "Jupiter evolving: transforming google's datacenter network via optical circuit switches and software-defined networking," Proc. of SIGCOMM, 2022, 10.1145/3544216.3544265.
12) P. M. Seiler et al., "56 GBaud O-band transmission using a photonic BiCMOS coherent receiver," 2020 European Conf. on Optical Communications (ECOC), 2020, 10.1109/ECOC48923.2020.9333218.
13) P. M. Seiler et al., "Toward coherent O-band data center interconnects," Front. Optoelectron. **14**, 414 (2021).
14) T. Gui et al., "Real-time demonstration of homodyne coherent bidirectional transmission for next-generation data center interconnects," J. Lightwave Technol. **39**, 1231 (2021).
15) P. M. Seiler et al., "Multiband silicon photonic EPIC coherent receiver for 64 GBd QPSK," J. Lightwave Technol. **40**, 3331 (2022).
16) L. Zimmermann, K. Voigt, G. Winzer, K. Petermann, and C. M. Weinert, "C-band optical 90°-hybrids based on silicon-on-insulator 4 × 4 waveguide couplers," IEEE Photon. Technol. Lett. **21**, 143 (2008).
17) K. Voigt, L. Zimmermann, G. Winzer, H. Tian, B. Tillack, and K. Petermann, "C-Band optical 90° hybrids in silicon nanowaveguide technology," IEEE Photon. Technol. Lett. **23**, 1769 (2011).
18) T. Pinguet et al., "High-volume manufacturing platform for silicon photonics," Proc. IEEE **106**, 2281 (2018).
19) A. Mekis et al., "A grating-coupler-enabled CMOS photonics platform," IEEE J. Sel. Top. Quantum Electron. **17**, 597 (2011).
20) S. Plantier, D. Fowler, K. Hassan, O. Lemonnier, and R. Orobtchouk, "Impact of scattering element shape on polarisation dependent loss in two dimensional grating couplers," 2016 IEEE 13th Int. Conf. on Group IV Photonics (GFP), Shanghai, China, p. 76, 2016, 10.1109/GROUP4.2016.7739057.
21) D. Taillaert, "Grating couplers as interface between optical fibres and nanophotonic waveguides," Ph.D. Thesis University of Ghent (2005).
22) F. van Laere et al., "Nanophotonic polarization diversity demultiplexer chip," J. Lightwave Technol. **27**, 417 (2009).

and Exhibition on Optical Communication (ECOC), 2013, 10.1049/cp.2013.1441.

23) G. Georgieva and K. Petermann, "Analytical and numerical investigation of silicon photonic 2D grating couplers with a waveguide-to-grating shear angle," 2018 Progress in Electromagnetics Research Symp. (PIERS-Toyama), 2018, p. 921, 10.23919/PIERS.2018.8598162.

24) G. Georgieva, K. Voigt, C. Mai, P. M. Seiler, K. Petermann, and L. Zimmermann, "Cross-polarization effects in sheared 2D grating couplers in a photonic BiCMOS technology," Jpn. J. Appl. Phys. **59**, SOOB03 (2020).

25) G. Georgieva, K. Voigt, P. M. Seiler, C. Mai, K. Petermann, and L. Zimmermann, "A physical origin of cross-polarization and higher-order modes in two-dimensional (2D) grating couplers and the related device performance limitations," J. Phys.: Photon. **3**, 035002 (2021).

26) L. Verslegers et al., "Design of low-loss polarization splitting grating couplers," Adv. Photon. Commun., 2014, paper JT4A.2, 10.1364/IPRSN.2014.JT4A.2.

27) J. Zou, Y. Yu, and X. Zhang, "Two-dimensional grating coupler with a low polarization dependent loss of 0.25 dB covering the C-band," Opt. Lett. **41**, 4206 (2016).

28) Y. Sobu, S.-H. Jeong, and Y. Tanaka, "Si-wire two-dimensional grating coupler with polarization-dependent loss of lower than 0.3 dB Over a 60 nm-wide spectral range," Jpn. J. Appl. Phys. **57**, 112501 (2018).

29) B. Chen et al., "Two-dimensional grating coupler on silicon with a high coupling efficiency and a low polarization-dependent loss," Opt. Express **28**, 4001 (2020).

30) G. Georgieva, P. M. Seiler, C. Mai, K. Petermann, and L. Zimmermann, "2D grating coupler induced polarization crosstalk in coherent transceivers for next generation data center interconnects," 2021 Optical Fiber Communications Conf. and Exhibition (OFC), paper W1C.4, 2021, 10.1364/OFC.2021.W1C.4.

31) Y. Luo et al., "Low-loss two-dimensional silicon photonic grating coupler with a backside metal mirror," Opt. Lett. **43**, 474 (2018).